Study on the light insulator between scintillator crystals

Hideki KOTAKA
Souichirou AOGAKI
Ikuo MORITANI
Fujio TAKEUTCHI*
Fumiharu Masafumi TOYAMA
Department of Information and Communication Sciences, Koto Sangyo University
**Faculty of Science, Kyoto Sangyo University*

Abstract

In our current project, we undertake an R&D of a new type of PED device which can be produced with a much lower cost yet has a better spatial resolution, compared to the currently used devices. In the course of this development, we encountered a difficulty of light cross-talk between the scintillator crystals. Large amount of effort has been paid to find out the best material to be used to reduce this cross-talk without reducing the light output and the spatial resolution. The experimental result shows that a black flock paper has the most promising features.

1. Introduction

The positron-emission tomography (PET) device is expensive. This factor, although the device is known to be useful in cancer therapy and brain science study, prohibits the device from becoming popular. In the current project, we try to establish a method to read out scintillator crystals using wave-length shifter (WLS) which should allow us to make the PET device with a much lower cost, and also to use much smaller crystals in a large number to obtain a better spatial resolution of the image [1]. The current setup used in this project is shown in Fig. 1. We use LYSO scintillator crystals (1 mm × 1 mm × 20 mm) to detect the gamma rays. The photons produced inside the crystal are transported to the end of the crystal, mainly by total reflection, and then transferred to wave-length shifter (WLS) used as light guide in order to lead the photons to position-sensitive photomultiplier (PSPM), a device which convert photons to electric signal. Inside a scintillator, until the light reaches the end of the long crystal, it has to be reflected many times inside the crystal, and for that reason, the transmission of the light by the total reflection

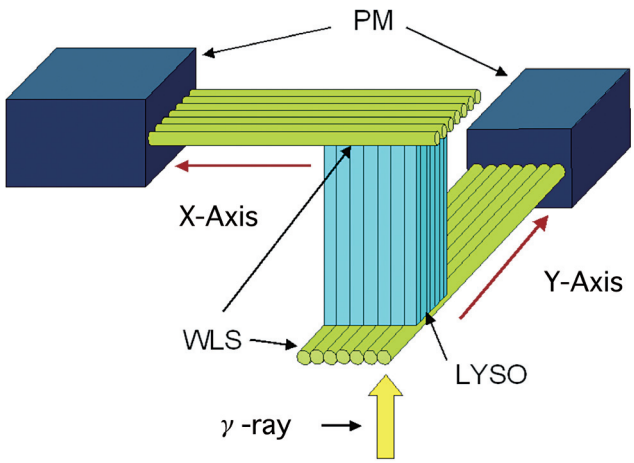

Fig. 1 Schematic view of a detector. Gamma-ray arriving from the bottom of the figure is absorbed by one of the 16 × 16 scintillator crystals forming the detector pad, and then many photons are emitted from the impact point into all directions. A part of the photons emitted reach the end of the long crystal after being totally reflected many times at the surface of the crystal, and again, only a part of them exit from the end point into the direction of WLS. WLS, after absorption of a photon, is chemically excited, and reemits another photon into a random direction. Thus WLS is used as a light guide to lead part of the light from the crystal to the photomultiplier. One WLS reads out 16 crystals and is connected to a channel of the 16 channels PSPM.

mechanism seemed the best way for the efficient transmission. The result of a simulation using EGS [2] for the event generation of the light transmission we made assuming the crystal to be a perfect rectangular parallelepiped with mirror surfaces indicates that,

1) among the emitted photons, only those which have relatively small angle with respect to the central axis of the crystal are transported to the end because the refractive index of the crystal is much higher than 1,
2) photons emitted with a large angle w. r. t. the central axis are either ejected outside the crystal, or stay inside the crystal, and can never exit from the end,
3) photons ejected from the side of a crystal can enter another crystal, but the direction of the propagation is conserved, and thus can never exit from the end of a crystal.

From these facts, we assumed that even without any insulating material of the light, the cross-talk between crystals can never occur. From the view point of increasing the effective volume (the fraction of the volume occupied by the scintillator within a detector) of the scintillator also, it is advantageous not to have any layer between the crystals.

However, in our process of repeating the experiments, we encountered phenomena in which the above-mentioned assumption is not correct. One of them is the size of the cross-talk. The cross-talk can also originate from the Compton scattering, thus it always exists to some extent, but

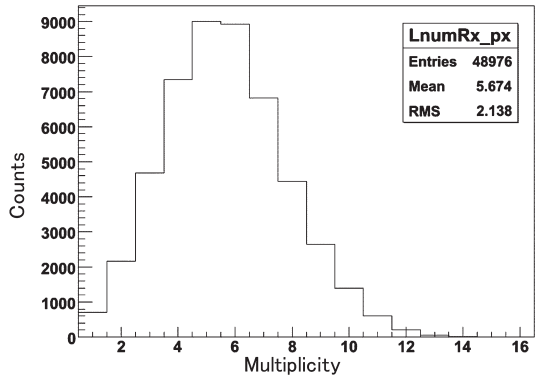

Fig. 2 The multiplicity distribution when there is no insulator material between the crystals. Multiplicity means number of WLS fired within an event when the detector pad consists of 16 × 16 scintillator crystals. PSPM H6568MOD was used.

as shown in Fig. 2, the multiplicity, that means the number of crystals firing in one event within a pad of 16 × 16 crystals, or rather the number of WLS firing, is often much larger than one.

Fig. 2 shows thus the multiplicity, and according to it, the average number of WLS which fire at a time is about 5.7. This is surely too large to assume that this phenomenon is due to the Compton scattering of the gamma-ray inside a detector pad. Thus this contradicts the simulation result. To explain this phenomenon one can imagine that the air layer between crystals disappears. In our experiment, the pad of crystals which have flat surfaces are pressed from outside by a frame in aluminum. Thus crystals are in complete contact, and the layer of air needed for the total reflection can be lost. If this assumption is right, we need to insert some material which keeps the distance between the crystals, and separate the surfaces. (It is already known experimentally that coating of the surface of the crystals leads to a very poor result.) Thus it is necessary to find a material which is thin yet which does not stick to the surface of the scintillator crystal. Opacity would also be desirable. We looked for candidates for that material and tested to find the best-suited material.

Insertion of any material certainly increases the volume of the pad, and it influences the effective volume. We consider this effect also in this study.

2. Candidate materials

Four materials have been tested in this study.

A. Flock paper (0.25 mm thick), black

B. Flock paper (0.11 mm thick) Golden river Mizoguchi, black

C. Tyvek (0.15 mm thick), a non-woven tissue developed by Dupond as building material. This has a milky white color, and is very stiff. It is used often for making envelopes etc. Also this material is often used as reflector in the field of nuclear experiment. It is an excellent reflector, but has a smooth surface, and thus might not be ideal to keep the air layer.

D. Teflon sheet (0.075 mm thick), white

A, B and C were inserted as grill walls surrounding crystal pieces. As for D, Teflon sheet, each crystal was wrapped with 3 layers of this material, and then a pad was built with this. In this case, the air layer might be hardly kept. The reason why the flock paper was chosen is it has a rough surface and one can expect it not to make a close contact with the crystal surface.

3. Experimental setup, and circuit used

Detector setup is roughly sketched in Fig. 1. In this experiment, we used LYSO as scintillating crystal. The main physical properties of LYSO crystal is shown in Table 1.

Table 1 Physical properties of the scintillator used

Name of the scintillator	L (Y) SO : Ce
Composition	Lu_2SiO_5
Refractive index	1.82
Density	7.35 g/cm^3
Effective Z	66.4
Decay time	40 ns
Photons emitted	27000/MeV
Wave length	440 nm

To match to the wave length of the crystal, Kuraray Y-11 WLS[3] was used. Its absorption spectrum has a maximum at 430 nm.

The size of the output signals from the PSPM are digitized by using ADC's, and the timing of them are recorded using TDC's connected after discriminators. The detail of the circuit used is explained in Appendix A.

It is important to estimate the effect of the insulation material to the amount of light yield and spatial resolution. Thus we chose a set up which allows to measure at the same time the spatial resolution and the cross talk. The spatial resolution measurement was done in 2 ways. First, in front of the detector pad, a collimator made of tungsten with a slit of 0.5 mm was placed between the radioactive source (^{22}Na) and the detector. This way, the gamma rays are localized as a narrow beam, and hit only one array of crystals in a pad, and from the response of the detector, the

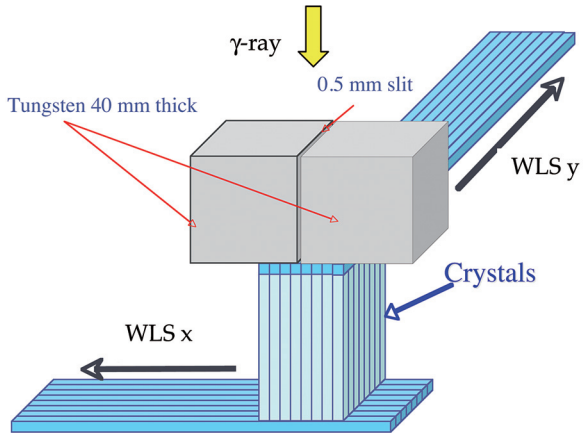

Fig. 3 Schematic view of a set up for the measurement of the spatial resolution using one detector. In this figure, the radioactive source is placed above the crystal pad. A tungsten collimator having a slit of 0.5 mm slit is placed between the detector and the radioactive source, just in front of the pad.

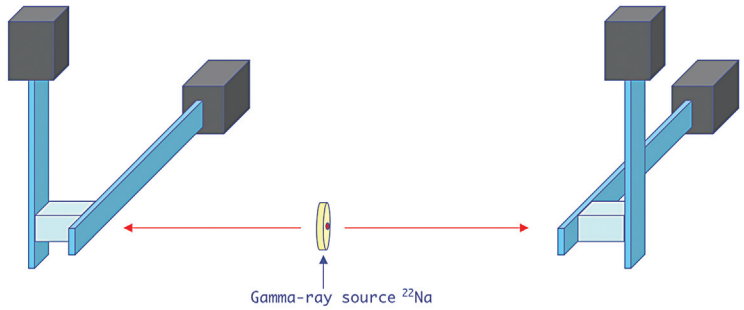

Fig. 4 Schematic view of the set up with two detectors used for the measurement of the spatial resolution. The radioactive source is placed in the middle of the disk in the center.

effective spatial resolution can be estimated. This set up is schematically shown in Fig. 3. In the second, two detector pads were symmetrically placed with respect to the radioactive source. In this way, the correlation of the hits between any pair of crystals, one in the first detector pad, and the other in the second detector pad was measured, and from that the effective spatial resolution was estimated. This set up is schematically shown in Fig. 4. In both cases, the distance from the source to the front side of the detector pad was 12 cm. However, as the Lutetium in the scintillator crystal has a natural radioactivity, even in the first measurement, another large NaI (Tl) detector was placed on the other side of the source, and the measurement was done in the coincidence.

In the present measurement, two kinds of PSPM were used. One is the traditional 16 channel metal tube made by Hamamatsu (H6568MOD). The other is a new type of the same PSPM,

but having a photocathode whose quantum efficiency is almost doubled compared to H6568MOD. The new PSPM is called H6568MODIII.

4. Measured quantities, Results

4.1 Multiplicity

We call the WLS array on the front side of the crystal pad, facing to the radioactive source the "y-side", and the opposite side the "x-side". With 2 cm long crystals, 70% of the 511 keV gamma rays are absorbed. But the absorption rate exponentially decreases with the depth. Thus one can expect a larger pulse height in average from the y-side. The time window between y-side and x-side signals was set to 10 ns. We took only events within this time window. Also in the coincidence measurement of two detectors, the timing window between the two detectors was set to 10 ns. Only events within those time windows were analyzed.

The multiplicity is defined as number of crystals fired within one event, but for the practical point of view, we measure rather the number of WLSs fired in an event.

A. Flock paper (0.25 mm thick), black

H6568MODIII PSPM was used for the readout. The result is shown in Fig. 5. The multiplicity is clearly reduced compared to the case without insulator. The average multiplicity is about 3.4.

B. Flock paper (0.11 mm thick) Golden river Mizoguchi, black

H6568MODIII PSPM was used for the readout. The result is shown in Fig. 6. The multiplicity is slightly larger than in the case of A, but clearly reduced compared to the case of no insulator.

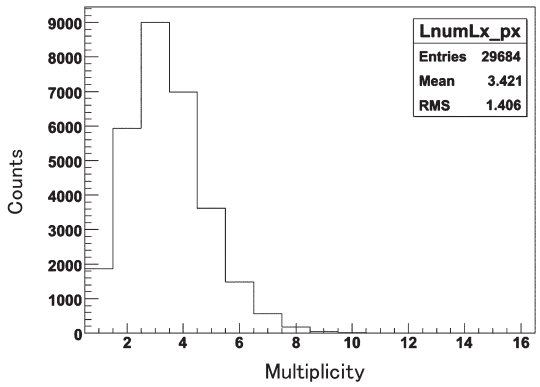

Fig. 5 Multiplicity distribution when the material A, the black flock paper (0.25 mm thick) was used as insulator between crystals. H6568MODIII was used as PSPM for the readout.

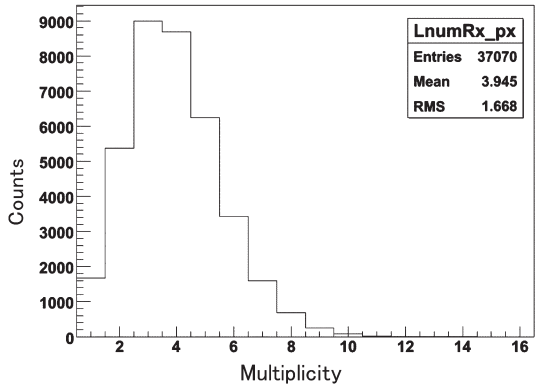

Fig. 6 Multiplicity distribution when the material B, the black flock paper (Golden river Mizoguchi 0.11 mm thick) was used as insulator between crystals. H6568MODIII was used as PSPM for the readout.

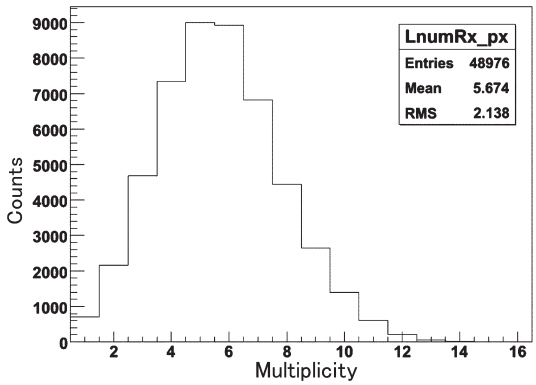

Fig. 7 Multiplicity distribution when the material C, Tyvek (0.15 mm thick) was used as insulator between crystals. H6568MODIII was used as PSPM for the readout.

The average multiplicity is about 3.9.

C. Tyvek (0.15 mm thick)

The result of the measurement is shown in Fig. 7. The average multiplicity is 5.7, and thus not very different from the case of no insulator.

D. Teflon sheet (0.075 mm thick)

The result is shown in Fig. 8. The average multiplicity which is 4.8 is slightly better than in the case without insulator.

From these results, we can conclude that the flock paper functions fairly well. The multiplicity is not expected to be affected by the type of PSPM.

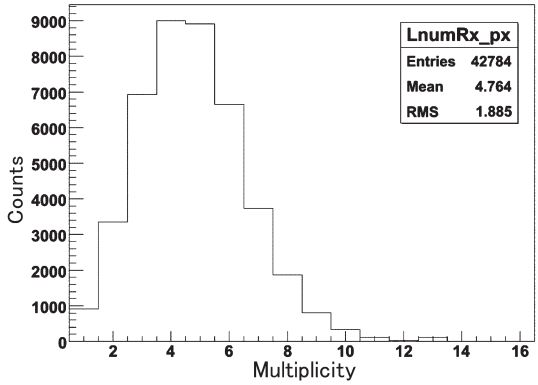

Fig. 8 Multiplicity distribution when the material D, Teflon sheet (0.075 mm thick) was used as insulator between crystals. H6568MODIII was used as PSPM for the readout.

4.2 Amount of light

In this measurement, we focus our attention to the amount of light from the last dynodes, and also the amount from each anode. A typical pulse-height distribution (ADC signal) from the anodes as well as that of the Last dynodes are shown in Figs. 9 and 10 respectively. In Fig. 10, the signal from the anode giving the largest signal among the multiple anodes fired is recorded. By the method explained here, we obtained the average number of photoelectrons and showed in Table 2. In this measurement, traditional PSPM, H6568MOD was used. As for the last dynodes, the average numbers of photoelectrons are

x 6.29,

y 6.17.

Table 2 Pulse-height from each anode when there is no light insulator, their average and the standard deviation.

No insulator					
Column number	Average photoelectrons		Column number	Average photoelectrons	
	x	y		x	y
1	7.68	5.50	9	8.53	7.15
2	6.49	5.39	10	7.86	7.45
3	7.12	6.02	11	7.96	7.47
4	4.57	6.33	12	7.26	7.28
5	6.36	6.50	13	6.80	7.72
6	8.81	6.66	14	7.26	8.63
7	9.31	6.85	15	7.24	9.23
8	8.82	7.16	16	7.76	9.76
			Average	7.49±1.12	7.19±1.18

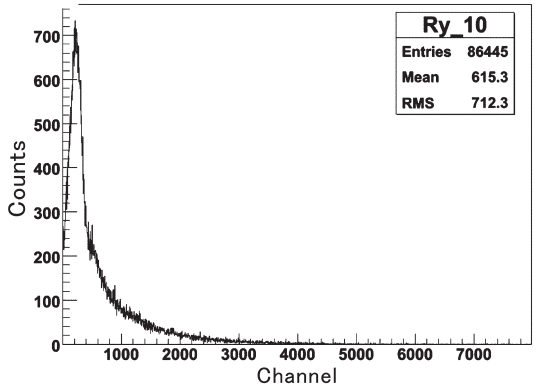

Fig. 9 Typical pulse-height distribution of the anode signals (y-side) when the insulator material is missing.

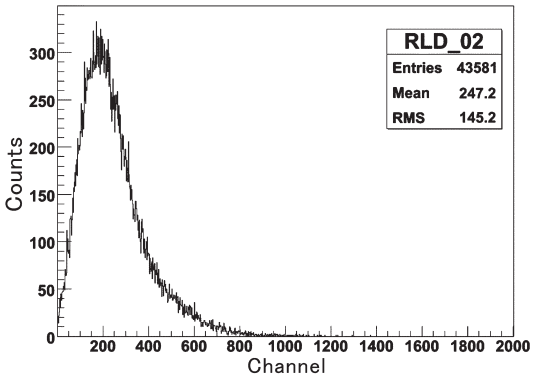

Fig. 10 Typical pulse-height distribution of the Last-dynode signals (y-side) when the insulator material is missing.

A. Flock paper (0.25 mm thick), black

The measurement was first done with the traditional PSPM, H6568MOD. The numbers of photoelectrons observed from each anode are shown in Table 3. As for the last dynodes, the average numbers of photoelectrons are

x 4.09

y 6.30.

Table 3 Pulse-height from each anode when the material A, flock paper (0.25 mm thick) was used as light insulator. Their average and the standard deviation.

A Flock paper (0.25 mm thick)					
Column number	Average photoelectrons		Column number	Average photoelectrons	
	x	y		x	y
1	6.72	9.01	8	5.60	7.73
2	6.46	7.73	9	4.23	5.38
3	7.23	8.44	10	5.47	5.79
4	7.02	8.76	11	5.14	6.25
5	5.06	8.10	12	5.77	7.89
6	4.92	7.78	13	7.04	8.47
7	5.36	7.59	Average	5.85±0.92	7.61±1.08

Then the pad was read out using a new PSPM, H6568MODIII for the sake of normalization. The results are shown in Table 4 and for the last dynodes, the average numbers of photoelectrons are

x 15.78

y 14.15.

Table 4 Average pulse-height from each anode when the material A, flock paper (0.25 mm thick) was used as light insulator. Their average and the standard deviation. PSPM used was H6568MODIII

Flock paper (0.25 mm thick)					
Column number	Average photoelectrons		Column number	Average photoelectrons	
	x	y		x	y
1	13.45	19.95	8	14.43	12.13
2	15.20	18.21	9	13.49	25.44
3	14.69	14.63	10	12.41	19.10
4	10.87	10.12	11	13.49	8.09
5	13.85	18.60	12	14.94	8.80
6	12.06	10.54	13	16.91	19.69
7	21.28	9.09	Average	14.39±2.47	14.95±5.33

B. Flock paper (0.11 mm thick) Golden river Mizoguchi, black

The pad was read out using a new PSPM, H6568MODIII. The results obtained for the anodes are shown in Table 5. As for the last dynodes, the average numbers of photoelectrons are

x 15.20

y 14.73.

Table 5 Average pulse-height from each anode when the material B, flock paper (0.11 mm thick) was used as light insulator. Their average and the standard deviation. PSPM used was H6568MODIII.

Flock paper (0.11 mm thick)					
Column number	Average photoelectrons		Column number	Average photoelectrons	
	x	y		x	y
1	8.31	10.94	8	9.93	13.05
2	8.90	10.31	9	10.7	9.74
3	9.42	8.46	10	9.09	8.17
4	8.86	11.34	11	9.42	8.28
5	10.08	9.58	12	10.35	9.47
6	11.28	8.98	13	9.48	12.15
7	10.42	9.12	14	9.10	10.26
			Average	9.67±0.80	9.99±1.41

C. Tyvek (0.15 mm thick)

The pad was read out using a new PSPM, H6568MODIII. The results obtained for the anodes are shown in Table 6. As for the last dynodes, the average numbers of photoelectrons are

x 22.53

y 22.44.

Table 6 Average pulse-height from each anode when the material C, Tyvek was used as light insulator. Their average and the standard deviation. PSPM used was H6568MODIII.

Tyvek					
Column number	Average photoelectrons		Column number	Average photoelectrons	
	x	y		x	y
1	10.06	14.61	8	13.02	13.50
2	11.18	15.90	9	15.36	16.88
3	12.17	15.42	10	12.78	13.76
4	11.87	12.55	11	12.50	11.13
5	13.66	16.30	12	13.63	12.00
6	14.42	11.92	13	11.21	13.96
7	13.30	12.44	14	11.73	19.46
			Average	12.68±1.39	14.27±2.23

D. Teflon sheet (0.075 mm thick)

The pad was read out using a new PSPM, H6568MODIII. The results obtained for the anodes are shown in Table 7. As for the last dynodes, the average numbers of photoelectrons are

x 18.19

y 18.39.

Table 7 Average pulse-height from each anode when the material D, Teflon sheet was used as light insulator. Their average and the standard deviation. PSPM used was H6568MODIII.

Teflon					
Column number	Average photoelectrons		Column number	Average photoelectrons	
	x	y		x	y
1	8.41	12.17	8	11.32	12.51
2	9.57	10.96	9	13.29	9.96
3	10.55	8.86	10	10.44	8.12
4	10.26	13.12	11	10.89	8.02
5	12.36	8.20	12	11.11	8.88
6	13.50	9.54	13	9.39	12.12
7	12.00	9.74	Average	11.01±1.50	10.17±1.81

All the above results are summarized in Table 8. We can notice that in fact the new PSPM H6568MODIII has almost two times larger quantum efficiency than the traditional H6568MOD as advertised by Hamamatsu. As far as the insulating material is concerned, the flock paper A is slightly superior, and flock paper B is slightly inferior to others.

Table 8 Summary of the light output when different materials are used as light insulator. The light output is indicated in terms of number of photoelectrons. As for anodes, average of multiple anodes and their standard deviation are shown.

	No insulator	A Flock paper	A Flock paper	B Flock paper	C Tyvek	D Teflon
Pspm used	MOD	MOD	MODIII	MODIII	MODIII	MODIII
Anodes x-side	7.49±1.12	5.85±0.92	14.39±2.47	9.67±0.80	12.68±1.39	11.01±1.50
Anodes y-side	7.19±1.18	7.61±1.08	14.95±5.33	9.99±1.41	14.27±2.23	10.17±1.81
Last dynode x-side	6.29	4.09	15.78	15.20	22.53	18.19
Last dynode y-side	6.17	6.30	14.15	14.73	22.44	18.39

4.3 Spatial resolution

Measurement with a collimator

The measurement was first carried out by using a tungsten collimator of 4 cm thick having a slit of 0.5 mm.

A. Flock paper (0.25 mm thick), black

Only a row of crystals in the pad are expected to be irradiated in this measurement. Thus ideally signals are populated in only one WLS in the histogram. However, the light cross-talk makes this single peak wider, and this results in a degradation of observed spatial resolution. A histogram of anodes fired is fitted with a gaussian and a constant background. The width of the

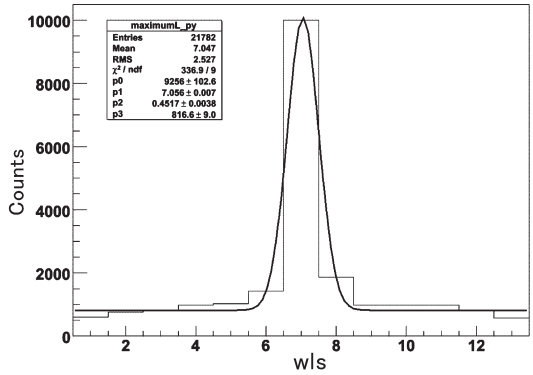

Fig. 11 Histogram of the reconstructed events as a function of the anodes (WLS). As insulator, material A, the black flock paper (0.25 mm thick) was used. H6568MODIII was used as PSPM for the readout.

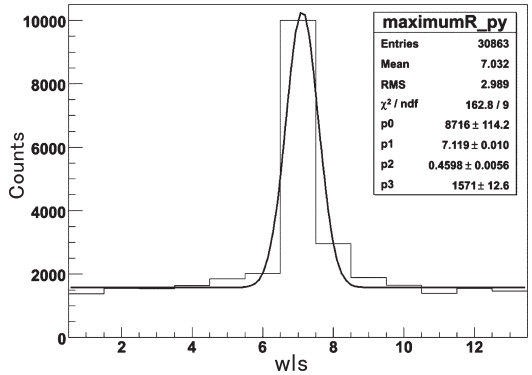

Fig. 12 Histogram of the reconstructed events as a function of the anodes (WLS). As insulator, material B, the black flock paper (Golden river Mizoguchi 0.11 mm thick) was used. H6568MODIII was used as PSPM for the readout.

gaussian is used as an indicator of the spatial resolution. Fig. 11 shows such a histogram for this readout using H6568MODIII. The width (RMS) of the gaussian is 0.45 crystals. Originally without insulator, the crystals are spaced with a constant step of 1 mm, but due to the insulator, the steps are larger. Thus this resolution is expressed in terms of "distance" as 0.556 mm in RMS.

B. Flock paper (0.11 mm thick) Golden river Mizoguchi, black

The pad was read out using H6568MODIII. The y-side anode histogram as well as its fit are shown in Fig. 12. The width of the peak (RMS) was 0.46 crystals, which corresponds to 0.525 mm.

C. Tyvek (0.15 mm thick)

The pad was read out using H6568MODIII. The y-side anode histogram as well as its fit are shown in Fig. 13. The width of the peak (RMS) was 0.55 crystals, which corresponds to 0.624 mm.

D. Teflon sheet (0.075 mm thick)

The pad was also read out using H6568MODIII. The y-side anode histogram as well as its fit are shown in Fig. 14. The width of the peak (RMS) was 0.493 crystals, which corresponds to 0.607 mm.

From the results shown above, we can conclude that the multiplicity and the spatial resolution are correlated. Insulator A gives the best result of fit, but due to its thickness, the overall resolution in terms of distance is better with B.

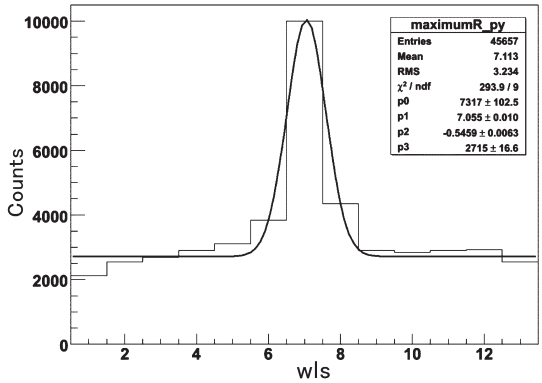

Fig. 13 Histogram of the reconstructed events as a function of the anodes (WLS). As insulator, material C, Tyvek (0.15 mm thick) was used. H6568MODIII was used as PSPM for the readout.

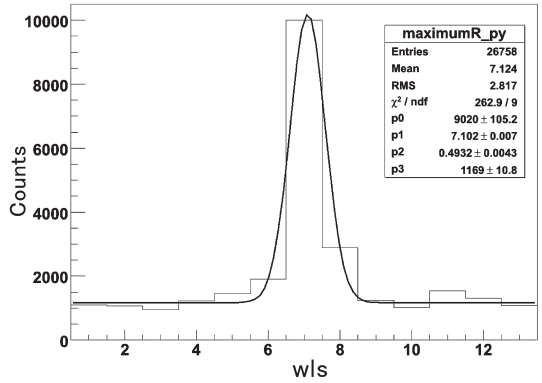

Fig. 14 Histogram of the reconstructed events as a function of the anodes (WLS). As insulator, material D, Teflon sheet (0.075 mm thick) was used. H6568MODIII was used as PSPM for the readout.

Coincidence measurement

We explained that the measurement using a slit is easily executed, and the result obtained (width) should be good as an indicator of the spatial resolution. However, we tried to measure the spatial resolution, which should allow one to estimate how much small distance in terms of difference in source position can be detected. For that, we have to make a coincidence measurement using two pads. We wished to use a pair of pads both having the insulator B which showed the best performance so far, but due to the availability of the materials, we had to concent on the coincidence measurement using pads with insulator A and D.

Fig. 15 explains the quantity so-called "shift" *s*. If the source is as small as a point, and there is no light cross-talk in the pad, if one gamma hits the R1 crystal, the other gamma should hit L 8 if the alignment is perfect. In that case if L6 fires in stead of L8, we define shift s to be 8 - 6 = 2. We detect all coincident events, and record the shift *s* in x-plane and y-plane. The result is shown in Fig. 16 as a two-dimensional histogram of (*sx*, *sy*). There are a considerable amount of accidental coincident events, which irradiate evenly the surface of the pads. However, due to the finite opening of each pad, these accidental coincident events are distributed shown a triangular shape in terms of shift *s*.

Fig. 17 shows the projection of Fig. 16 to the x-axis. The histogram was fitted with a gaussian and a triangular background. The RMS width of the gaussian is 1.12 mm. With a simple simulation, one can deduce that the actual spatial resolution above-mentioned is about half of the width of the shift. Thus the result indicates that the ultimate spatial resolution should be about 0.6 mm RMS and 1.4 mm FWHM.

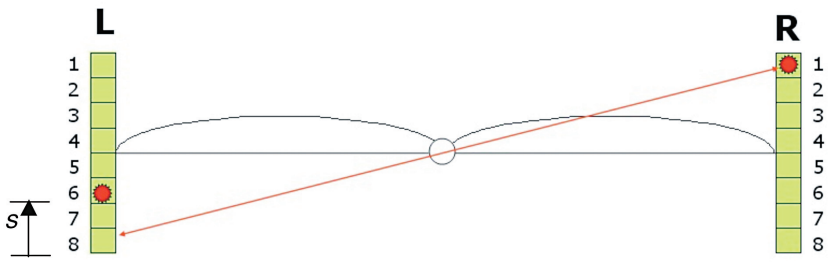

Fig. 15 The definition of the shift "*s*" used as an indicator for the spatial resolution when it was measured with two detectors in coincidence. Assume that one gamma-ray is detected with scintillator 1 in the right detector (R), the scintillator 8 in the left detector (L) is assumed to fire in coincidence, when the source is just point-like, and the spatial resolution is very good. If, in reality the crystal 6 fires in stead of 8 in the detector L, then *s* is defined as 6 - 8 = -2. In the text, the numbering of the crystals (WLS) is different.

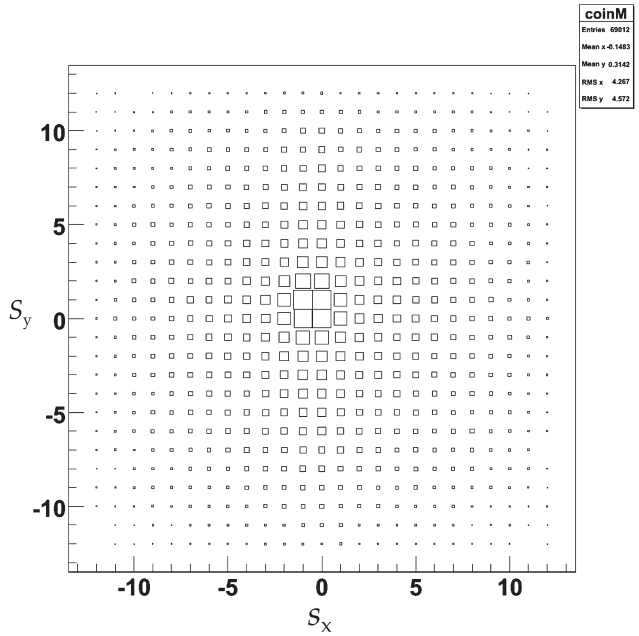

Fig. 16 Two-dimensional histogram of the shifts (*sx*, *sy*) when the 2 detectors using insulator material A (flock paper 0.25 mm thick) and D (teflon), respectively were used for the measurement.

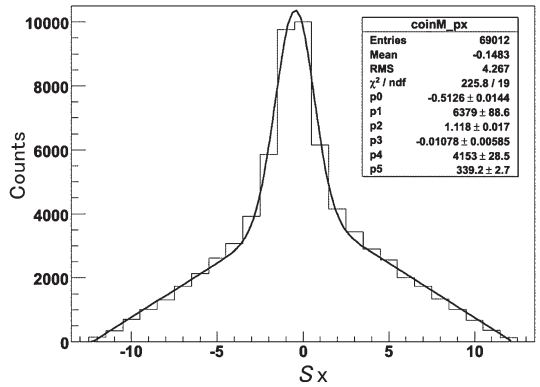

Fig. 17 Projection of the 2-dimensional histogram shown in Fig. 16 to the x-axis, and its fit using a gaussian peak and a triangular background (see text).

5. Conclusions

It became clear that the high multiplicity is due to the light cross-talk, and the insertion of light shielding material reduces it. The cross-talk is caused mainly by the lack of air layer between the crystals. To avoid the direct contact, we studied several materials to be inserted between the crystals. Tyvek, tellon tape, thick and thin black flock papers have been tried out.

The comparison was made from the view point of the multiplicity, light yield and the spatial resolution. The spatial resolution was measured by using a collimator having a thin slit.

The result showed that the flock paper gives by far the best result as far as the multiplicity is concerned. From the view point of the light yield, the flock paper A is slightly superior, and the flock paper B is slightly inferior to others. But as the thickness of flock paper A is two times larger than that of B, it is difficult to adopt A as a standard material to be used in the future from the view point of the effective volume. The spatial resolution is strongly correlated with the multiplicity. The flock paper A gives the best result in terms of distance in number of crystals, but in the distance in mm, flock paper B is superior. From this study, we concluded that the most promising shielding material to be used in the future is flock paper B. The thickness of this material is 0.11 mm, thus 11% of the crystal. This is translated as a loss of effective volume by 22%, which is non-negligible. It is therefore necessary to continuously look around and seek for a better material in the future.

Appendix

A. The circuit used for the experiment

The signals coming from the PSPM are transferred to the computer through a logical circuit and a CAMAC interface. Fig. A1 shows a sketch of the circuitry to read out one detector (one pad), and the central coincidence unit which is surrounded by a dotted line. The former part exists as many as the number of detectors to be used in one measurement. The central coincidence unit also makes an interrupt signal which is a trigger signal for the data acquisition. Fig. A2 shows the rough sketch of the last dynode signals. The present circuit is optimized to the measurement of such signals. In the current explanation, the number of photoelectrons yielded from the last dynode is assume to be several. As the PSPM is fast, the last dynode signal, which is the sum of anode signals looks like a chain as shown in the first and the third row. These pulses are more frequent immediately after the absorption of the gamma-ray by the crystal, then reduced with the life time of the crystal (In our case of LYSO, the life time is about 40 ns). To measure precisely the light yield, one has to integrate this signal for about two times the decay time. On

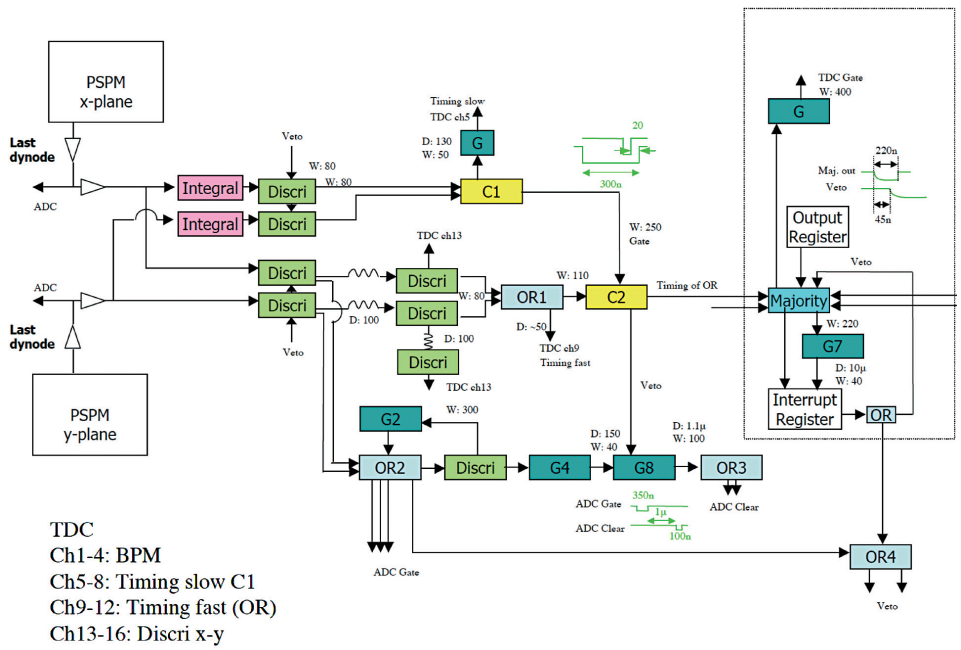

Fig. A1 Schematic presentation of the circuitry used when the measurement was executed with multiple detectors. The figure shows only the part related to one detector (this part exists as many as the number of detectors), and the single common part relative to the coincidence and the data acquisition in the dotted rectangle. See text for the detail.

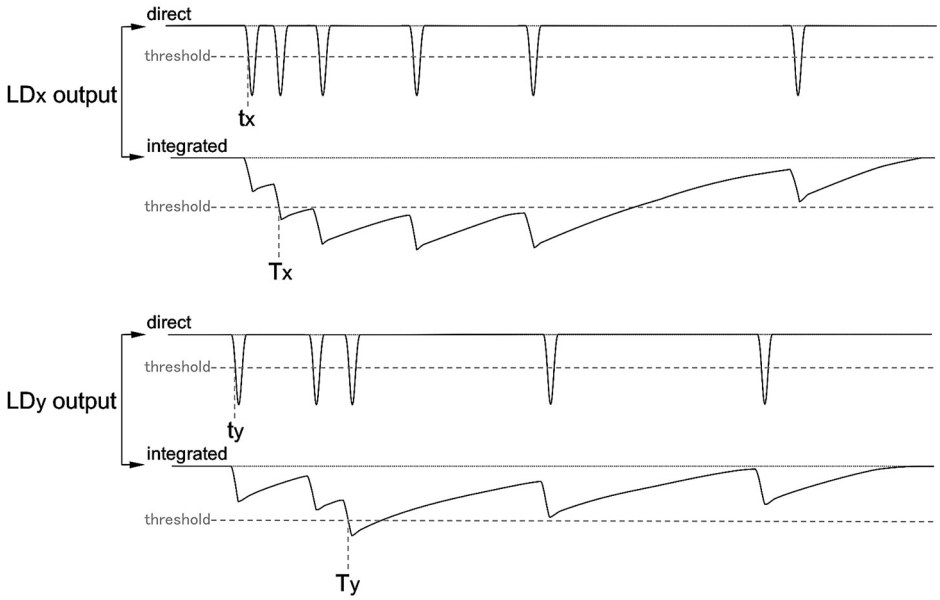

Fig. A2 Schematic view of the last-dynode signals LDx and LDy, and the explanation of the timings used in the text. The last-dynode signals are split into 2 parts, and one of them is integrated before going to the discriminator with a time constant of several nanoseconds.

the other hand, we integrate this signal with a time constant of several nanoseconds in forder to generate a trigger signal. This signal is shown in the second and the fourth row. We feed a discriminator with this integrated signal, and set a threshold at a level of 2 – 3 photoelectrons (about 20 mV) so that the small noises are dropped. We denote the timing of the discriminators output by Tx and Ty. We also feed a discriminator with the direct signal, and set a threshold level for one photoelectron. We denote the timing of this discriminator output with tx and ty. The earliest signal which is related with the absorption of a gamma-ray is formed with an OR of the direct lines (OR1 in the figure). Let us call the timing of this signal TOR. This is determined by the earlier of tx and ty. The gate of the ADC should be opened with this signal (which is formed with OR2 in the figure). The width of the gate is set to about 80 ns, which is two times the decay time of the crystal used (fixed by the gate generator G2). The capture of the gamma-ray is announced by the coincidence of the integrated line (C1). Let us call the timing of this signal Tcoinc.

When there are several detectors, we need to use an overlap of the coincidence signals of the integrated line. However, the signal provided by C1 contains a too large jitter, and it is necessary to use the timing TOR. When there is no coincidence, the signal TOR is just a noise. Thus we delay this signal by a fixed amount and then gate it with a real coincidence signal using C2 signal. The integration starts at the timing of TOR in the ADC. But the the real coincidence is missing,

the ADC output is useless. Thus we generate a fast clear signal with OR3 and discharge the ADC in that case. When there are signals simultaneously from more than one detector, the trigger signal is formed with the Majority coincidence circuit, and the computer is interrupted, the data are transported to the computer. The computer is busy for several milliseconds. This busy signal (OR4) is distributed to all the discriminators and vetoes them to take a new event. The timing of signals at each level are digitized with the help of the TDC, and transferred to the computer through the Camac crate controller (CCC).

B. Measurement of the absolute value of the light output

The light output from the scintillating crystal must be measured in terms of number of photons, since the pulse-height resolution, timing etc. are all determined by the number of photons observed. As far as the PM is used for the reading of the photons, the number of photons is reduced by the quantum efficiency which is about 20% till now. This means the light output is quantized to about 5 photons which corresponds to 1 photoelectron. By measuring the output pulse from the PM integrated for the gate time, one cannot tell how many photoelectrons are recorded at the level of the photocathode, the input to the PM, since the gain of the PM is strongly dependent of the HV bias applied to it, and it is not easy to calibrate it.

There are, however, certain kind of PM which allows to measure the output signal corresponding to the single photoelectron. In these PM's, the electric field in the vicinity of the first dynode is well designed, and whatever the direction of the single photoelectron emitted from the photocathode, this produces a fixed amount of current at the anode. This has been a feature reserved to very expensive PMs which, when the light pulse is small, can produce output current for one, two, three,… photoelectrons distinctively. The PM we are using, Hamamatsu H6568 has this feature, namely when the light pulse height is several, it shows a peak corresponding to the single photoelectron, which is called single-photoelectron peak.

By using this feature, we can normalize the gain of the PM, and thus can tell how many photons are hitting the photocathode, or rather how many photoelectrons are produced at the photocathode within an event.

Fig. A3 shows a typical pulse-height distribution which is an ADC spectrum. ADC unit is normally positively biased. Thus to know the zero point, we give trigger signal, but without the input signal. The tiny and sharp peak at channel 1001 was produced this way. This spectrum was taken with a threshold relatively high to reject background. Now we lower the threshold of the discriminator, then the shape of the spectrum changes to something similar to what is shown in Fig. A4. One starts seeing a peak at channel 1020, since there is not input signal to the PM smaller than

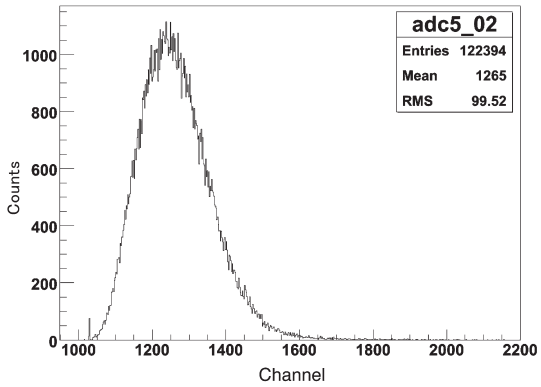

Fig. A3 A typical pulse-height spectrum obtained with ADC. One can see that the average of the spectrum is 1265 (channels).

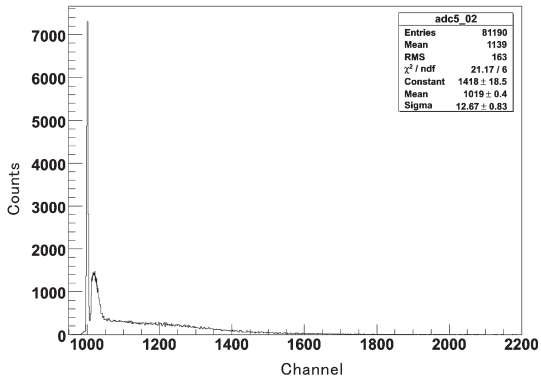

Fig. A4 Same ADC spectrum as in Fig. A3. The discriminator threshold for the corresponding channel is lowered in the trigger to obtain this spectrum. A pedestal peak is also added just by switching momentarily the trigger to random. By fitting the single-photoelectron peak, the peak position is found to the 1019 channels while the pedestal is at 1001 channels.

one photoelectron. The position of the single-photoelectron peak is fixed to 1019 by the Gaussian fit, then one can calibrate the gain of the PM to

$$1019 - 1001 = 18 \text{ (channels)}$$

for a single photoelectron. The average number of channels of the peak in Fig. A3 is 264 assuming that channel 1001 corresponds to zero point. Now dividing 264 by 18, one can find that the light output corresponds to 14.67 photoelectrons. If one assumes a quantum efficiency of 20%, this corresponds to 73 photons as the average input to the PM.

The quantum efficiency of the head-on type PM has been about 20% for bialkali for a very long time. Recently Hamamatsu started to produce a special photocathode which has 2 times higher quantum efficiency. We introduced a new kind of PSPM in the present study which has

this new photocathode and named H6568MODIII.

References

[1] F. Takeutchi and S. Aogaki; Read-out of a YAP array detector using wave-length shifter, Proc. Intern. mini-Workshop for Scintillating Crystals and their Applications Nov. 2003, KEK Japan (2004) 213-218,
F. Takeutchi and S. Aogaki; Read-out of scintillator crystal matrix using wave-length shifter, Proceedings of the Eighth International Conference on Inorganic Scintillator and their Use in Scientific and Industrial Applications, SCINT2005 at Crimea, Sept. 2005. Proceedings pp 298-302,
F. Takeutchi and S. Aogaki; Development of a High-resolution Fast Gamma-ray Imager for the New-generation PET, Bull. Res. Inst. Advanced Tech., Kyoto Sangyo University Vol. **4** (2005) 45 - 68,
K. Inoue et al.; Development of a High-resolution Fast Gamma-ray Imager for the New-generation PET II, Bull. Res. Inst. Advanced Tech., Kyoto Sangyo University Vol. **5** (2006) 97 - 124,
F. Takeutchi and S. Aogaki; Read-out of YAP and LuYAP crystal matrix using wave-length shifter, Bull. Res. Inst. Advanced Tech., Kyoto Sangyo University Vol. **5** (2006) 85 - 96
S. Aogaki et al.; Development of a High-resolution Fast Gamma-ray Imager for the New- generation PET III, Bull. Res. Inst. Advanced Tech., Kyoto Sangyo University Vol. **6** (2007) 65 - 82

[2] EGS, http://www.slac.stanford.edu/egs/

[3] Catalog Kuraray Japan